Supplementary Information for

From separation to photothermal conversion: selective crystallization of thorium from lanthanides

Junpu Yang,[a] Yaoyao Bai,[a] Guangtao Zhang,[a] Jingqi Ma,[a] and Jian Lin*,[a]

[a]School of Nuclear Science and Technology, Xi'an Jiaotong University, Xi'an 710049, PR China. *jianlin@xjtu.edu.cn

Experimental Procedures

Materials and Synthesis

Caution! *Caution! Th-232 used in this study is an emitter with the daughter of radioactive Ra-228. All of the thorium compounds used and investigated were operated in an authorized laboratory designed for actinide element studies. Standard protections for radioactive materials should be followed.*

Materials. $Th(NO_3)_4 \cdot 6H_2O$ (99.9%, Changchun Institute of Applied Chemistry, Chinese Academy of Sciences), 1-pyrene carboxylic acid (Hpca) (RG, 98%, Bide Pharmatech Ltd.), CF_3COOH (GC, 96%, TCI (Shanghai) Development Co., Ltd.), and dimethylformamide (99.5%, Shanghai Macklin Biochemical Co., Ltd) were used as received from commercial suppliers without further purification.

Synthesis.

A mixture of $Th(NO_3)_4 \cdot 6H_2O$ (0.01 mmol), 1-pyrene carboxylic acid (Hpca) (0.01 mmol), CF_3COOH (60 μL), DMF (200 μL), and deionized water (800 μL) were loaded into a 7 mL glass vial. The vial was sealed and heated to 100°C for 72 h and then cooled to room temperature under ambient conditions. Brown acicular single crystals of **Th-pca** were obtained. The crystals were washed with ethanol and dried under ambient conditions.

Characterizations

Single-crystal X-ray diffraction (SCXRD) analyses were conducted on a Bruker D8-Venture single crystal X-ray diffractometer equipped with an IμS 3.0 microfocus X-ray source (Mo–Kα radiation, λ= 0.71073Å) and a CMOS detector at 298 K. The collection and reduction of single crystal diffraction data were completed in *APEX3* program. The structures were solved by Intrinsic Phasing with *ShelXT* [S1] and refined with a full-matrix least-squares technique of ShelXL [S2] interpreted by *Olex2* [S3]. The Bruker D8 Advance diffractometer (40 kV, 40 mA) with Cu Kα radiation (λ = 1.54060 Å) was used to collect powder X-ray diffraction (PXRD) patterns in steps of 0.02°. The simulated PXRD pattern of **Th-pca** was generated from their CIF using the Materials Studio. The X-ray photoelectron spectroscopy (XPS) spectra were obtained using a Thermo Scientific Escalab 250Xi spectrometer, with measurements conducted at binding energies ranging from 0 to 1350 eV. Scanning electron microscopy images coupled with energy dispersive X-ray spectra of **Th-pca** were collected using a MAIA3 LMH field emission scanning electron microscope from TESCAN. The UV-Vis-NIR absorption spectra of **Th-pca** was obtained using a PE Lambda950 spectrometer, with measurements conducted on powder samples across a wavelength range of 300–1500 nm. The electron paramagnetic resonance (EPR) measurements were performed on a Bruker A300 spectrometer. The EPR spectrum of **Th-pca** was recorded at room temperature and the microwave power used was 1.0 mW. The photoluminescence spectra were measured using an Edinburgh FLS980 fluorescence spectrometer at room temperature. The thermogravimetric analysis (TGA) was investigated on a Waters SDT650 simultaneous thermal analyser. The experiments were conducted in a dry N_2 atmosphere at a temperature range of 30-800 °C with a heating rate of 10 °C/min.

Selectivity crystallization Study

In a typical synthesis, $Th(NO_3)_4 \cdot 6H_2O$ (0.1 mmol), $Ln(NO_3)_3 \cdot 6H_2O$ (Ln = La, Eu, or Yb) (0.1 mmol), Hpca (0.1 mmol), and CF_3COOH (40 μL) were dissolved in 1 mL of H_2O/DMF (v/v = 4:1) in a 7 mL sealed vial and heated at 100 °C for 3 days.

For the Th/Eu and Th/Yb systems, the solid and liquid phases were separated by filtration, followed by determination of Th(IV) and Ln(III) concentrations in both phases.

For the Th/La system, after separating the solid and liquid phases by filtration, the solid product was further treated by dissolving **Th-pca** in DMF. The dissolved solution was filtered. The concentrations of Th(IV) and La(III) in DMF solution and the remaining solid phase were then analyzed.

The concentrations of Th(IV) in both the mother liquor and solid products, as well as Ln(III) in the mother liquor, were measured using inductively coupled plasma optical emission spectrometry (ICP-OES) (Thermo Fisher Scientific iCAP 7400). The concentrations of Ln(III) in the solid products were determined using inductively coupled plasma mass spectrometry (ICP-MS) (PerkinElmer NexION 350D).

Separation factors (SFs) were calculated using the following equation:

$$SF = ([Th]_{Solid}[Ln]_L)/([Ln]_{Solid}[Th]_L)$$

where $[Th]_{Solid}$ and $[Ln]_{Solid}$ are the concentrations (molar amounts) of thorium and lanthanide, respectively, in the solid phase. $[Th]_L$ and $[Ln]_L$ are the concentrations of Th(IV) and Ln(III) cations, respectively, in the liquor phase.

Photothermal Conversion Study

Finely ground samples (5 mg) were pressed into a 5 mm diameter pellets. The pellets were irradiated with an 808 nm laser with different powers. Temperature changes during the photothermal conversion were recorded using an InfReC R450D-pro infrared imager.

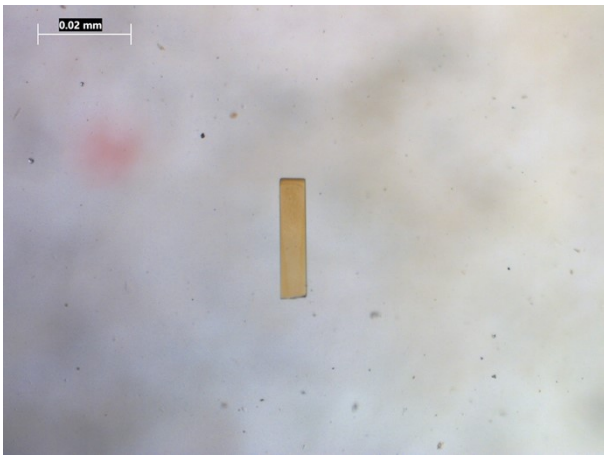

Fig. S1 Crystal image of **Th-pca**.

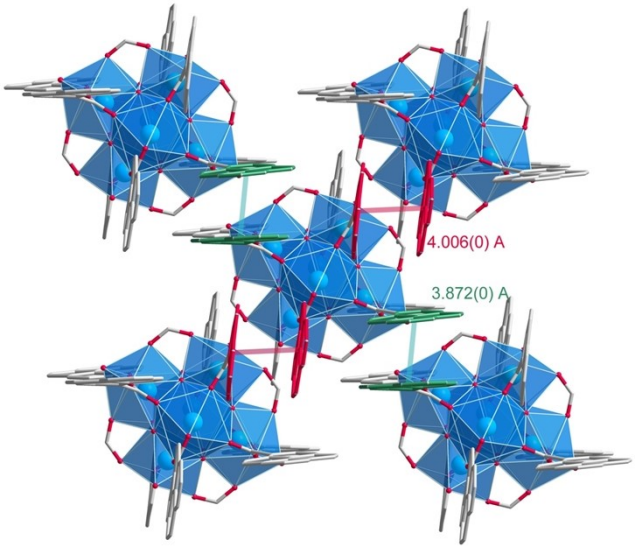

Fig. S2 Representation showing the π-π interactions between the neighbouring Hpca ligands in **Th-pca.**

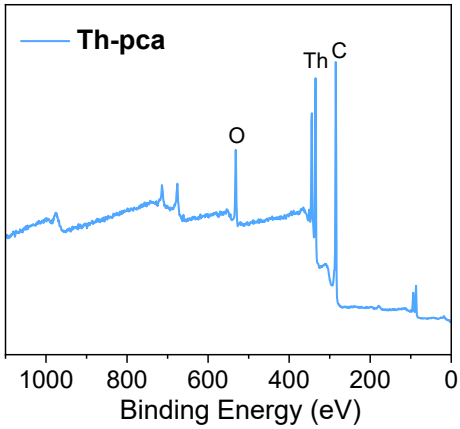

Fig. S3 X-ray photoelectron spectroscopy (XPS) spectrum of **Th-pca**.

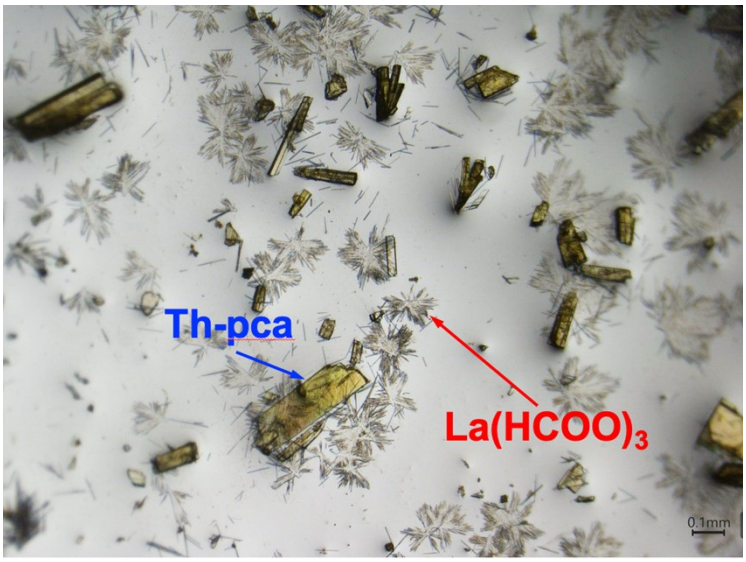

Fig. S4 Optical image showing the crystalline products of **Th-pca** and $La(HCOO)_3$ obtained from the La/Th system.

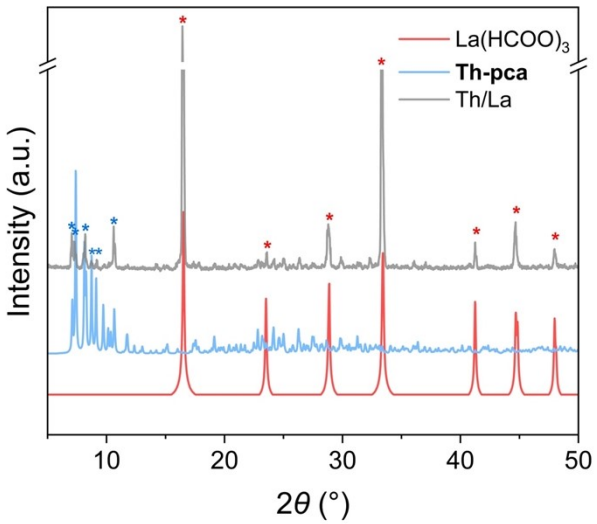

Fig. S5 PXRD pattern of the solid product from the La/Th system, compared with the simulated patterns of **Th-pca** and $La(HCOO)_3$.

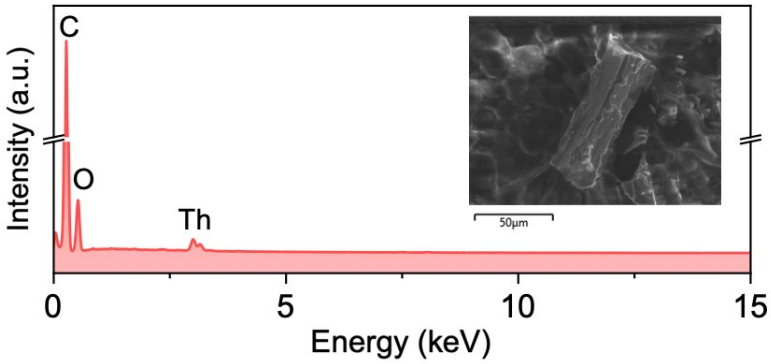

Fig. S6 SEM image and EDS spectrum of a crystal obtained from the Th/Eu system.

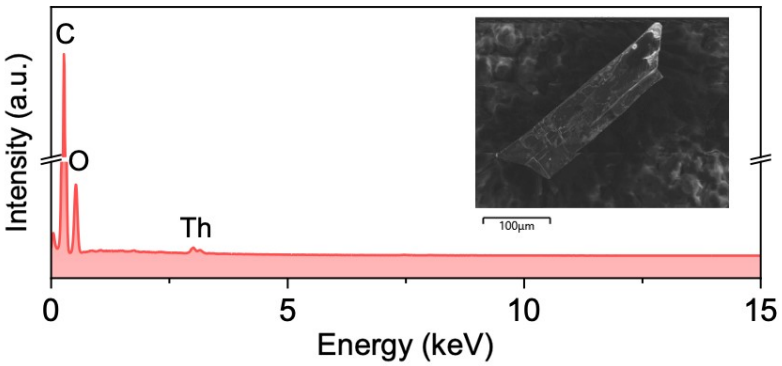

Fig. S7 SEM image and EDS spectrum of a crystal obtained from the Th/Yb system.

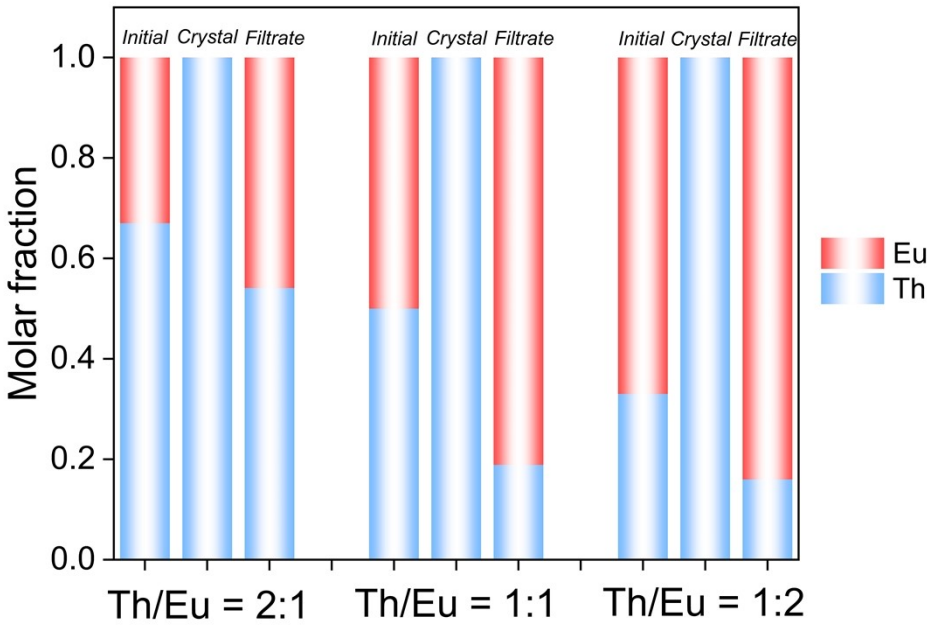

Fig. S8 Separation performance of the Th/Eu system under varying initial Th/Eu ratios. At Th/Eu initial ratios of 2:1, 1:1, and 1:2, the Th/Eu ratios in the filtrate were 1.18, 0.23, and 0.19, respectively.

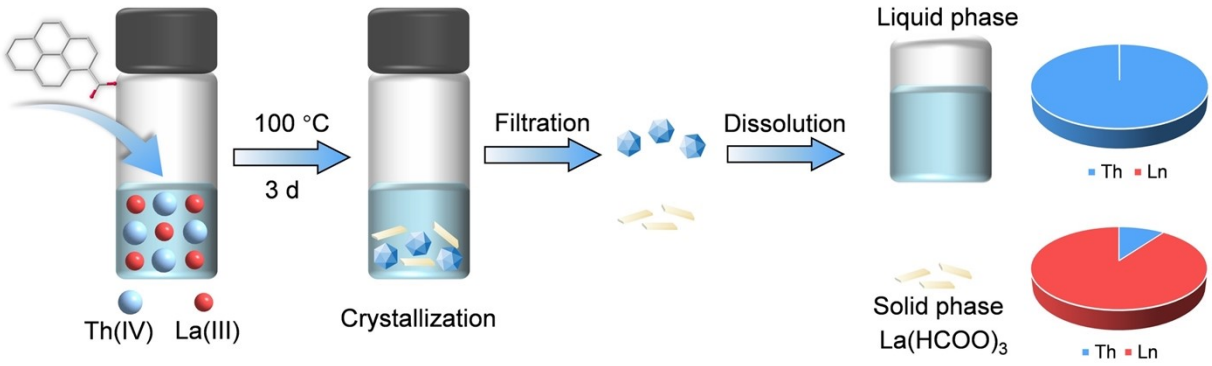

Fig. S9 Schematic representation showing the separation of Th(IV) and La(III) via selective crystallization and dissolution.

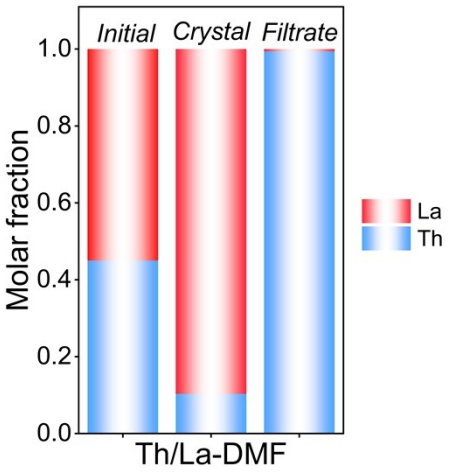

Fig. S10 Separation results from the Th/La system. The three bars, from left to right, represent the molar distribution of Th/Ln in the starting materials, solid products, and liquid phase, respectively.

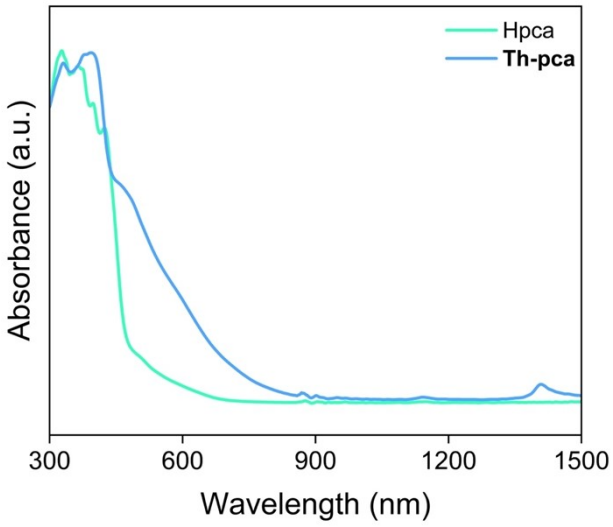

Fig. S11 UV-Vis-NIR absorption spectra of powder samples of Hpca and **Th-pca**.

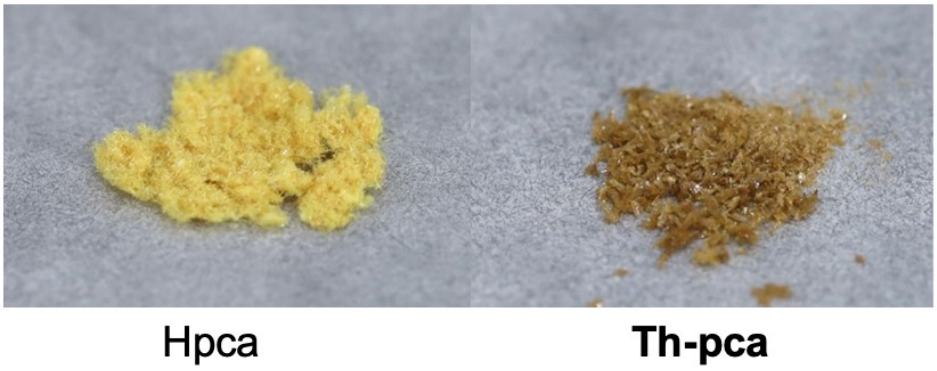

Fig. S12 Photographs showing the appearance of Hpca and **Th-pca** powder samples under ambient light.

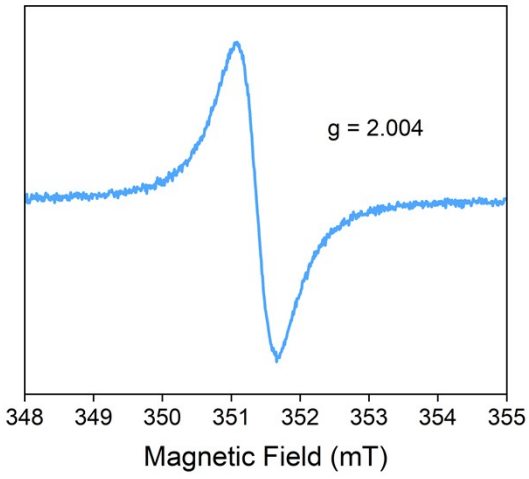

Fig. S13 EPR spectrum of as-synthesized **Th-pca**.

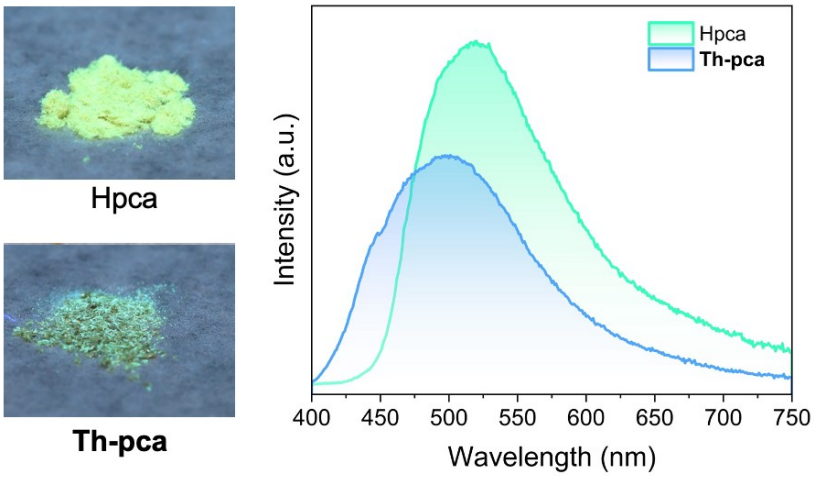

Fig. S14 Photographs and photoluminescence spectra (λ_{ex} = 365 nm) of **Th-pca** and Hpca under comparable irradiation conditions.

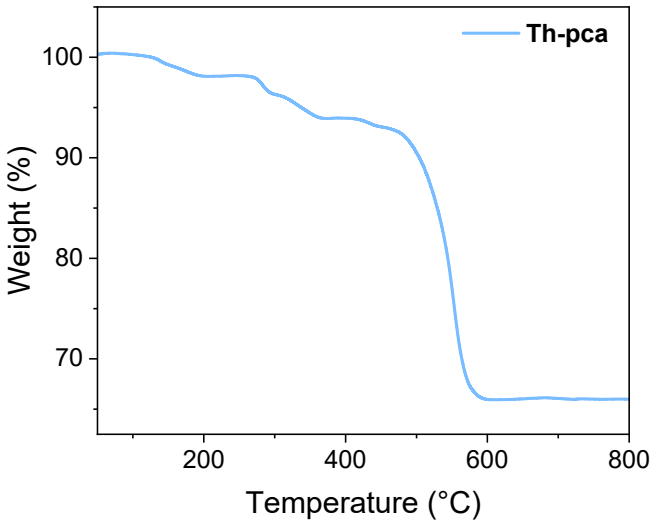

Fig. S15 Thermogravimetric analysis (TGA) curve of **Th-pca**.

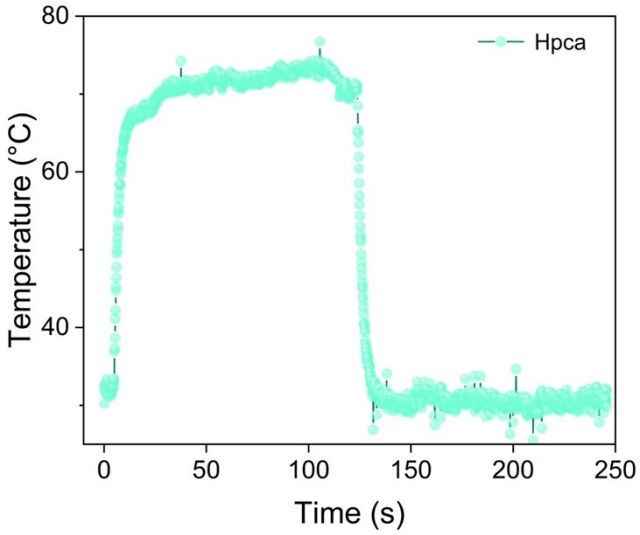

Fig. S16 Photothermal conversion curve for Hpca under 1 W 808 nm laser irradiation.

Table S1 Crystallographic data for **Th-pca**.

CCDC	2448605
Formula	$C_{70}H_{40}O_{18}Th_3$
Formula weight	1865.14
$\rho_{calc.}$ (g cm^{-3})	2.045
μ (mm^{-1})	7.424
Colour	Brown
Habit	Acicular
Space group	*P-1*
a (Å)	10.1687(4)
b (Å)	11.9584(5)
c (Å)	25.0200(9)
α (deg)	91.1790(10)
β (deg)	95.315(2)
γ (deg)	90.783(2)
V (Å^3)	3028.4(2)
Z	2
T (K)	298
λ (Å)	0.711
Θ_{max} (deg)	27.496
R_1	0.0251
ωR_2	0.0573
R_{int}	0.0354
GooF	1.020

Supplementary References

[S1] G. M. Sheldrick, *Acta Crystallogr. Sect. A: Found. Adv.* **2015**, *71*, 3.

[S2] G. M. Sheldrick, *Acta Crystallogr. Sect. C: Struct. Chem.* **2015**, *71*, 3.

[S3] O. V. Dolomanov, L. J. Bourhis, R. J. Gildea, J. A. K. Howard, H. Puschmann, *J. Appl. Cryst.* **2009**, *42*, 339.